ON THE STRENGTHENING OF THE CENTRIFUGALLY CAST HK40 TUBE

Md. Bahaa Zaghloul*, Takayuki Shinoda, and Ryohei Tanaka

Metallugical Engineering Dept., Tokyo Institute of Technology
Ohokayama, Meguro-ku, Tokyo, Japan, 152
*Graduate Student of Tokyo Institute of Technology
from the National Research Center of Egypt

ABSTRACT

This is offered as a contribution to the study of the strengthening mechanism of the centrifugally cast HK40 steel. The approach was to clarify the correlation between the structural factors and the creep rupture strength of HK40 steel. A suitable as cast structure for the higher creep rupture strength was obtained by controlling the cooling rate during the centrifugal casting, which promoted the larger dendrite cell structures. Both the secondary structure and the grain boundary morphology were controlled by the addition of Ti which induces the uniform precipitation of secondary carbides and the discontinuous grain boundary morphology, and by the addition of Nb which induces the fine precipitation of the lamellar carbides. The discontinuous and irregular boundary morphology and the lamellar carbides on the cell boundaries were found to be effective in retarding crack propagation during the tertiary creep period, causing an increase in creep rupture time. A combined addition of Ti and Nb to HK40 steel in the order $(Ti + Nb)/C \simeq 0.3$ and $Ti/(Ti + Nb) \simeq 0.3$, in atomic ratios, was found to be very effective in giving the suitable structure for the optimum creep rupture strength. The result was considered to be an extraordinarily high creep rupture strength for HK40 steel, superior to that of IN519 alloy. The improved Ti and Nb added HK40 steel, when compared at the same temperature, has a strength about 1.7 times higher than the plain HK40 steel, and, at an equal stress, it can be used at temperatures about 100°C higher than the plain HK40 steel.

Introduction

The centrifugally cast 25Cr-20Ni-0.4C austenitic steel (ACI HK40) is widely used at high temperatures in petrochemical plants. However, in order to achieve a high efficiency in petrochemical processes by increasing both temperature and pressure[1,2], improved cast materials having higher strength are strongly desired. Although there is considerable information now available on the structure and properties of HK40 steel[3,6], it is necessary to clarify the correlation between structural factors and creep rupture strength in order to obtain better creep rupture strength. This research work is aimed at contributing to the study of the strengthening mechanism of the centrifugally cast HK40 tubes in order to obtain the highest available strength. Three main strengthening factors--the primary cast structure, the secondary structure i.e. the inside grain precipitations, and the grain boundary condition--are the subject of this work. The first approach was to control the centrifugal casting condition, e.g. the cooling rate, to obtain a suitable primary structure. Then, under the best casting condition obtained the effect on the creep rupture strength of the addition of carbide forming elements such as Ti and Nb as structure controlling variables was investigated. The significant effect of single[7] and combined[8,9] additions of Ti and Nb on carbide dispersion and the high temperature strength of various kinds of austenitic steels has been established. In addition, the higher creep rupture strength of the modified HK40, i.e. IN519 alloy (25Cr-25Ni), was attributed to the addition of Nb[10,11]. The addition of Ti and Nb was useful with regard to the resistance to weld cracking in the heat affected zone of CK-20 castings (25Cr-20Ni)[12]. So, the combined addition of Ti and Nb was undertaken to improve the creep rupture strength of HK40 steel. Finally, the study was carried out on the grain boundary precipitation and morphology in relation to the void formation and crack propagation that lead to the creep fracture.

Experimental Procedures

All the experimental heats of this work were melted in a basic lined 15KVA high frequency induction furnace. The heats were centrifugally cast into a 5kg laboratory scale centrifugal casting machine to give a cast tube of 120mm length, 100mm outside diameter, and 20mm wall thickness. The first five heats were centrifugally cast under different cooling rates which were measured during the centrifugal casting in the Liquid+Solid range, by employing different types of molds (copper, cast-iron, and graphite); also two different centrifugal forces were applied, 70g and 100g (g is the acceleration of gravity). The other heats were cast under a fixed condition, employing a copper mold with 100g. The creep rupture tests and aging treatments were conducted at 950, 1000, 1050 and 1100°C in some cases; the aging periods were 100, 300 and 1000 hours. For all steels, creep rupture data was plotted to give the Larson-Miller master rupture curves. The X-ray identifications were carried out on the electrolytically extracted residues of primary and secondary precipitates. In addition, the lattice parameters of the as cast and aged specimens were measured using the Debye-Scherrer camera technique. Optical and electron microstructural observations were also conducted.

Results and Discussion

I The Relation Between The As Cast Structure And Creep Rupture Strength

The measured cooling rates as a result of changing the centrifugal casting condition together with the chemical compositions of the five heats are shown in Table I. As shown in the table, the tube cast into a graphite mold under 70g, G-7, has the lowest cooling rate, "204 degC/min"; however, the tube cast into a copper mold under 100g, C-10, has the highest cooling rate, "804 degC/min". Due to the differences in the cooling rates recorded in table I, there are considerable structural variations as shown in Fig.1 and Table II. It has

Table I

Chemical compositions of HK40 with the cooling rate according to casting condition

Specimen	Casting condition		Cooling rate degC/min	Chemical Composition, wt%		
	Mold type	Centrifugal force		C	Ni	Cr
G-7	Graphite	70g	240	0.35	20.0	24.4
G-10	Graphite	100g	384	0.36	20.7	24.6
CI-10	Cast Iron	100g	636	0.37	20.8	25.0
C-7	Copper	70g	-	0.36	20.3	24.9
C-10	Copper	100g	804	0.35	21.0	24.0

Si: 0.34∿0.45, Mn: 1.30∿1.44, N: 0.02∿0.08
S: 0.010∿0.012, P: 0.002∿0.003

Table II

Structural variations and creep rupture strength of HK40

Specimens	Volume fraction of carbide eutectic (%)	Lattice parameter of as cast (A)	Dissolved carbon content of as cast (wt%)	Mean size of dendrite cell (mm)	Creep rupture strength* (kg/mm^2)	
					1000°C 1000 hr	1000°C 10000 hr
G-7	5.03	3.5945	0.12	0.045	1.50	0.90
G-10	4.31	-	-	0.048	1.55	0.92
CI-10	3.44	3.5958	0.15	0.056	1.60	0.95
C-7	2.09	-	-	0.075	1.70	1.05
C-10	1.99	3.5962	0.17	0.093	1.75	1.15

* The creep rupture strength was calculated from regression equation.

been noticed that the tube with the lower cooling rate has a smaller size of columnar structure and a higher volume fraction of carbide eutectic, with subsequently a smaller amount of dissolved carbon, as estimated from the measured lattice parameter, than the tube with the highest cooling rate in the as cast condition. Also, the size of the dendrite cell structures, which appear by aging, is smaller for the G-7 tube than the C-10 tube. It is found that the creep rupture strength of the C-10 tube is higher than that of the G-7 tube, and the difference in the strength increases with the increase in the test temperature, as shown in table II. Fig.2 shows that the difference in the particle size of the secondary carbides diminishes with the increase in aging temperature. Hence, the dispersion strengthening by the secondary carbides does not contribute to the estimated difference in the strength at higher temperatures. Also the difference in the amount of dissolved carbon as estimated from the lattice parameters of the tubes in the as cast condition does not explain the difference in the strength, since all tubes have the same lattice parameter after aging. The size of the dendrite cell structures "d" was found

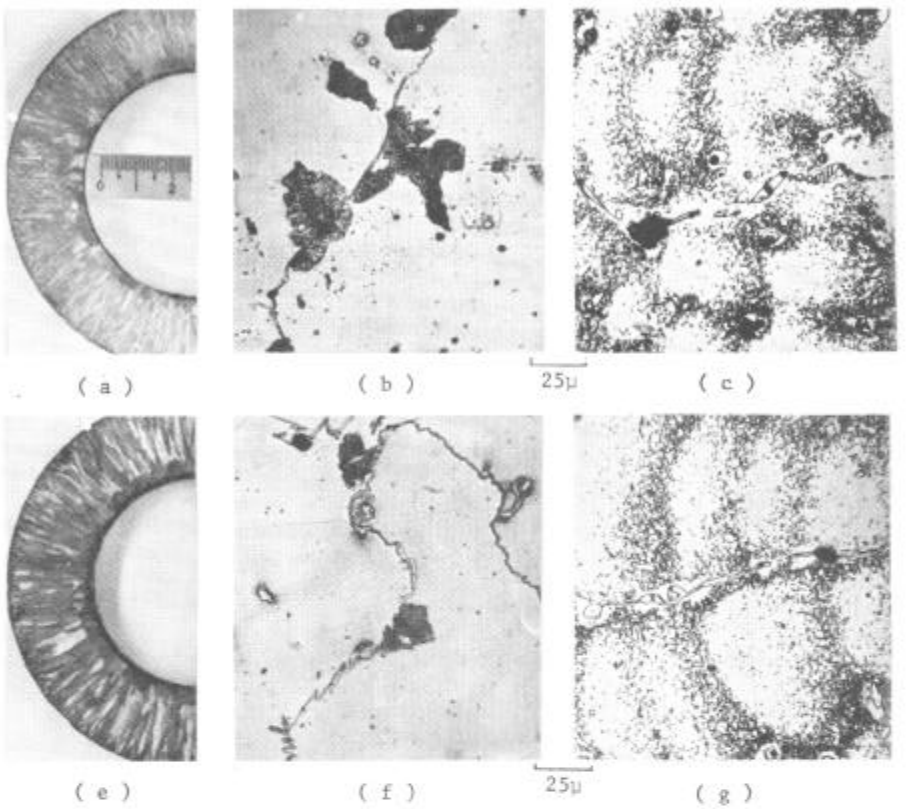

Figure 1: The macro-structure, as cast and aged microstructure of G-7 tube (a, b and c) and C-10 tube (e, f and g).

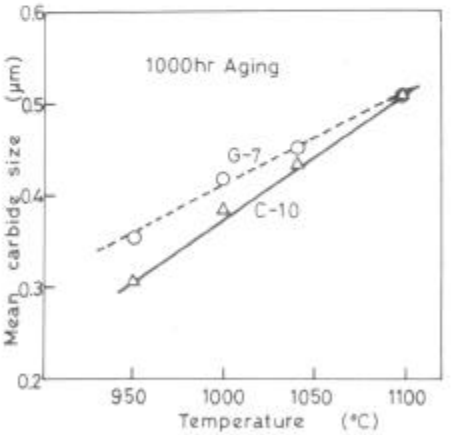

Figure 2: Changes in the mean particle size of precipitated carbides of G-7 and C-10 tubes with aging temperatures.

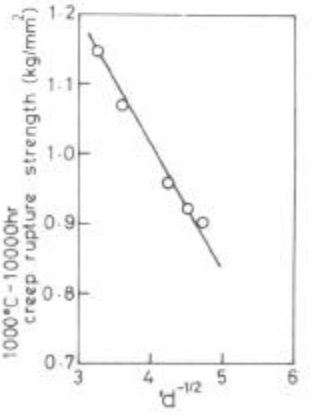

Figure 3: Dependence of creep rupture strength on the size of dendrite cell structure, d.

to be the most important factor contributing to the differences in the strength at higher temperatures. This is deduced from Fig.3 which shows that the creep rupture strength σ, at 1000°C-1000 hr is inversely proportional to the reciprocal root of dendrite cell structure size d, or $\sigma \propto -1/\sqrt{d}$. These results emphasize that a high cooling rate during the centrifugal casting of HK40 steel is necessary to promote a larger dendrite cell size for a higher creep rupture strength.

II Effect of Ti & Nb Additions on Structure and Creep Rupture Strength

In addition to enhancing the creep rupture strength of HK40 steel by obtaining a suitable cast structure through the control of the cooling rate during solidification, the creep rupture strength also can be improved by controlling the secondary structure, i.e. the type and morphology of secondary precipitated carbides. In view of the dispersion strengthening trend with carbide stabilizing elements, which are less soluble in the austenitic matrix and also induce different carbide morphologies, the work for improving the creep rupture strength of HK40 steel was undertaken by single and combined additions of Ti and Nb. The chemical composition of the heats is shown in Table III. The centrifugal casting condition was fixed, using a copper mold at 100g.

Table III

The chemical compositions of Ti and Nb added HK40 steels

Mark	C	Ti
T1	0.45	0.19
T2	0.44	0.24
T3	0.46	0.76
T4	0.31	1.76

Mark	C	Nb
N1	0.44	1.42
N2	0.45	1.74
N3	0.47	1.95
N4	0.53	3.60

Mark	C	Ti	Nb	(Ti+Nb)*/C	Ti*/(Ti+Nb)
K1	0.43	0.15	0.47	0.23	0.38
K2	0.44	1.13	1.15	0.97	0.66
K3	0.45	0.15	0.60	0.26	0.32
K4	0.45	0.15	1.75	0.58	0.14
K5	0.43	0.38	0.51	0.63	0.76
K6	0.46	0.71	1.15	0.71	0.55

Ni: 19.62∿20.51,
Cr: 24.11∿26.37,
Si: 1.28∿1.73, Mn: 1.29∿1 55
* atomic ratio.

II-1 Effect of Ti and Nb on the Structure

The addition of Ti and Nb to HK40 steel causes substantial changes in its structure. The microphotographs of the as cast and aged structures of 1.76%Nb added and 0.76%Ti added HK40 steels and 0.15%Ti + 0.60%Nb added HK40 steel are illustrated in Fig.4. It is obvious that the addition of Nb helps to form a considerable amount of the coarse lamellar type of carbide eutectic which forms an almost continuous network of dendrite cell structures. However, the Ti addition forms the lamellar type of carbide eutectic on grain boundaries with isolated islands of the coarse lamellar eutectic inside the grains which can be easily transformed into a massive type. The combined addition of both Ti and Nb, as shown in the photographs, forms a lamellar type of grain boundary carbide but coarser than those formed by the single addition of Ti and Nb. The results of X-ray analysis carried out on the extracted residues indicate that the carbide form in Ti added HK40 steel consists mainly of M_7C_3 and TiC. However, the Nb added steel has $M_{23}C_6$ and NbC up to 1.95%Nb and mainly NbC for the 3.6%Nb. The combined addition of Ti and Nb produced all the types of carbides mentioned above. After aging, the M_7C_3 type completely disappeared. The intensive fine precipitation of $M_{23}C_6$ carbides is shown in all steels after aging. The Ti added steel is distinguished by its uniform precipitation all over the matrix; however, in Nb added steel the carbide particles precipitate mainly on the dendrite cell boundaries. In addition, the coarsening of the

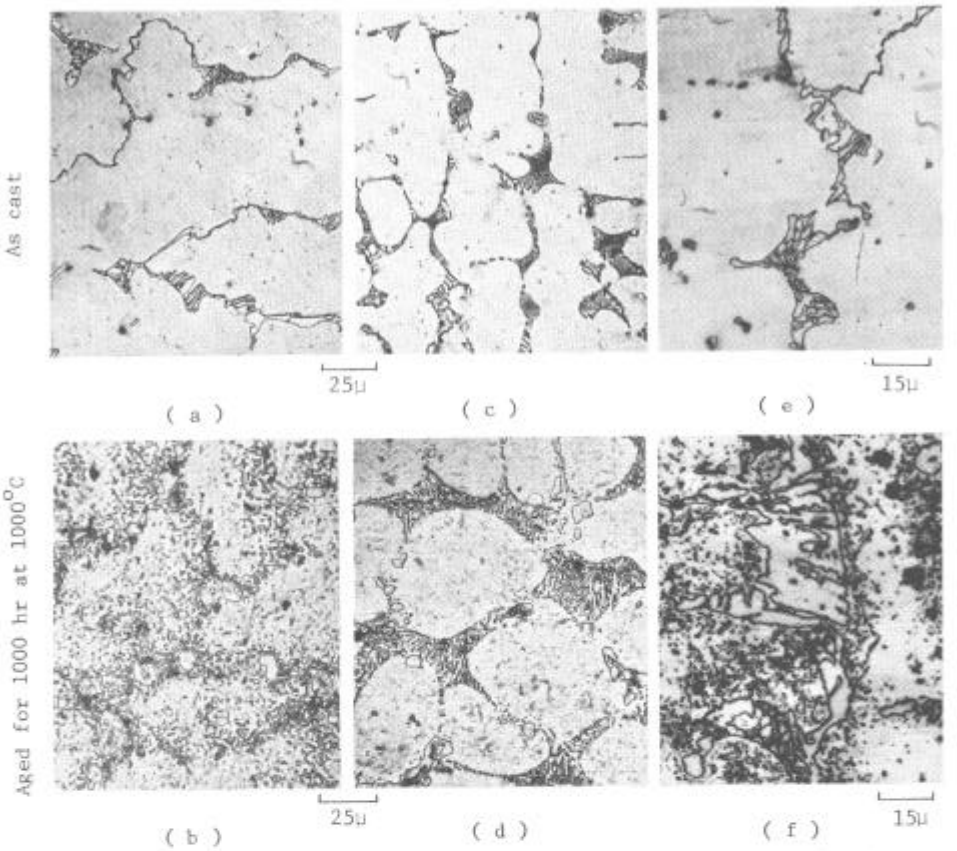

Figure 4: Microphotographs of 0.76%Ti (a and b), 1.74%Nb (c and d) and 0.15%Ti+0.6%Nb (e and f) added HK40 steels as cast and aged, respectively.

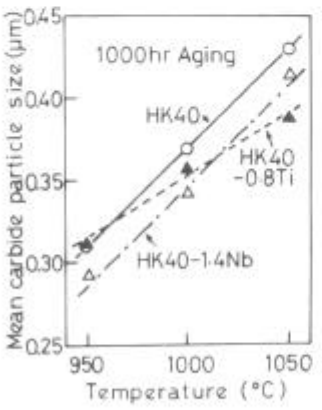

Figure 5: Changes in the mean particle size of precipitated carbides of HK40 and Ti and Nb added steels with aging temperatures.

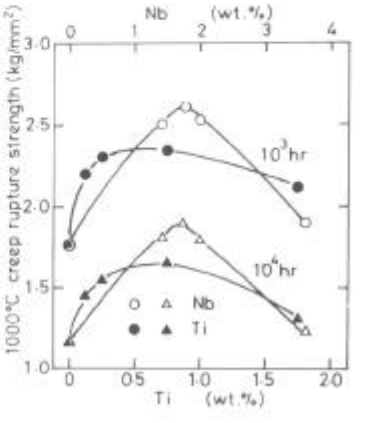

Figure 6: The creep rupture strength of Ti and Nb added HK40 steels in relation to the percent of addition.

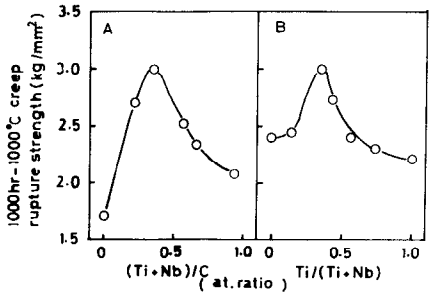

Figure 7: The creep rupture strength of Ti+Nb added HK40 steel in relation to (Ti+Nb)/C, (A) and Ti/(Ti+Nb), (B).

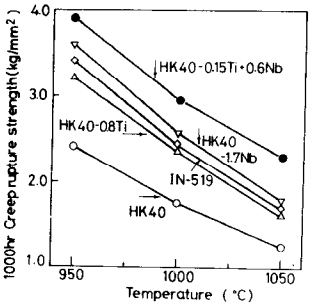

Figure 8: The creep rupture strength of HK40, Ti, Nb and Ti+Nb added HK40 steels together with IN519 steel at different temperature.

lamellar carbide eutectic of Ti added steel is completed after aging and forms in discontinuous isolated islands; meanwhile, the lamellar NbC of carbide eutectic remains even after a long period of exposure to higher temperatures. As regards the aged structure of the Ti and Nb added steel, it is to be noted that the secondary carbides are uniformly precipitated in the matrix in the same way as in the case of Ti added steel, which the grain boundary carbides become massive but with an irregular and complexed morphology. The changes in the particle size of carbides for Ti and Nb added steels as compared with plain HK40 steel, under the 1000 hr aging at 950°, 1000° and 1050°C, are shown in Fig.5. Although the carbides of Nb added steel are finer than those of Ti added steel at the lower temperature, they coalesce more easily with the increase in aging temperature; on the other hand, the carbides of Ti added steel remain finer at the higher temperature.

II-2 Effect of Ti and Nb Additions on Creep Rupture Strength

Although the constant "C" of the Larson-Miller parameter has been taken as 15 in the case of plain HK40 steel, this value is not suitable for steels with Ti and Nb additions. Through a regression analysis, a constant of 22 was found suitable for these steels. The 1000°C-1000 and 10000 hr inter- and extrapolated values from the master curves of Ti and Nb separately added steels are presented in Fig.6 in relation to the Ti or Nb addition. The remarkable increase in creep rupture strength of HK40 steel by Ti addition and in particular by Nb addition, irrespective of the creep time is obvious. The Nb added steel shows a peak in the strength at 1.74%Nb or Nb/C atomic ratio ≈ 0.5, while the strength drops with more Nb addition. In the case of Ti addition the higher strength is obtained by 0.76%Ti or Ti/C atomic ratio ≈ 0.5. As mentioned earlier, the Nb added HK40 steel is superior in its creep rupture strength to the Ti added one of the same atomic ratio of Nb/C or Ti/C ≈ 0.5. However, it was also estimated that at higher temperatures the secondary carbides in Nb added steel coalesce to higher degree than the Ti added one, which gives rise to the assumption that there might be a drop in the creep rupture strength of Nb added HK40 steel after extremely prolonged time or at higher temperatures. Meanwhile the uniform precipitation of secondary carbides caused by Ti addition may possibly maintain the strength at such conditions. Accordingly, the combined addition of Nb and Ti was done in order to utilize both of their advantages. The 1000°C-1000 hr inter-polated creep rupture strength of all steels with the combined additions of Ti and Nb as plotted against the respective atomic ratio of (Ti+Nb)/C and Ti/(Ti+Nb) is presented in Fig.7, A and B, respectively. As shown in Fig.7-A, the maximum creep rupture strength is obtained at the atomic ratio of (Ti+Nb)/C≈0.3 and an increase in this ratio is followed by

a decrease in the creep rupture strength. Increasing the ratio more than 0.3 means a decrease in the amount of the $M_{23}C_6$ secondary carbides which are considered important for dispersion strengthening. From Fig.7-B, it is shown that the maximum creep rupture strength is obtained at the atomic ratio of Ti/(Ti+Nb)≈0.3. Also, the creep rupture strength decreases with the increase in this ratio. This means that the creep rupture strength is more affected by the Nb addition which causes the lamellar eutectic; nevertheless, about one third of the total addition should be Ti in order to utilize the role of Ti in causing the uniform precipitation of secondary carbides. The inter- and extrapolated 1000 hr creep rupture strengths of all the steels in the present work at different temperatures, in comparison with IN519 alloy are shown in Fig.8. It is obvious that the 0.15%Ti+0.16Nb added steel is superior in its strength to IN519, and it has a strength about 1.7 times higher than the plain HK40 steel when compared at the same temperature, and at an equal stress, it can be used at temperatures about 100°C higher than the HK40 steel.

III Effect of Carbide Morphology on Creep Fracture

Metallographic examinations of creep ruptured specimens of the steels in the present investigation showed that the creep fracture occurs when numerous cavities or cracks, which form along the grain boundaries or on the interface between the massive carbides and the matrix, have grown and coalesced; this is in agreement with Mclean[13]. Hence, it was necessary to investigate the effect of different carbide morphologies created by the Ti and Nb additions on the creep fracture. In case of plain HK40 steel, since the grain boundary massive carbides form in continuous shapes, the cavities which form along these boundaries join easily, forming cracks which also propagate easily and yield to fracture. Therefore, the examination on cavity formation and crack propagation was undertaken on two steels having different morphologies. One is the discontinuous grain boundary carbides with the secondary carbides dispersed throughout the matrix of the Ti added HK40 steel; the other is the lamellar carbides intensively precipitated on the grain boundaries and dendrite cell boundaries. In these two models, the numbers of cavities and cracks was measured on several specimens crept for different periods distributed on the creep curve in different t_c/t_r ratios where t_c is the creep time and t_r is the total creep rupture time. Fig.9 represents the two creep curves of 0.8%Ti (ruptured after 150 hr) and 1.7%Nb (ruptured after 310 hr) in relation to the t_c/t_r ratios, for some of which the number of voids and cracks were counted as illustrated in the upper part of the figure. As shown in the figure, the voids increasingly form during the steady state creep period; and by the start of tertiary creep, these voids agglomerate and tend to form the cracks resulting in a decrease in the voids number and an increase in the cracks number. However, due to the discontinuous grain boundary morphology of the Ti added steel, the agglomerated voids in comparison with the plain HK40 steel, take a longer time to form the long cracks which yield to fracture, since the ratio t_{III}/t_r in Ti added steel and plain HK40 steel are 0.44 and 0.1, respectively, t_{III} is tertiary creep time. In the case of Nb

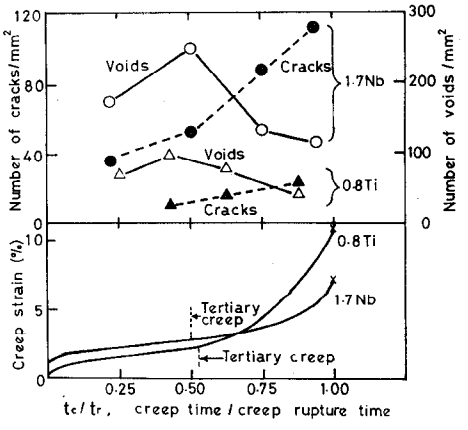

Figure 9: The number of voids and cracks of Ti and Nb added HK40 steels at different points on the creep curve of different t_c/t_r ratios, t_c is the creep time and t_r is the creep rupture time.

added steel, the voids form on the interface between the grain boundary carbides and the austenitic matrix; moreover a large number form on the tips of the fine lamellar carbide making the total number much higher than the case of Ti added steel. However, because the cracks, which are formed by the joining of voids, propagate through a looped path around and inside the lamellar cells, they last a longer time before yielding to fracture. Hence, the resulting long life creep rupture of Nb added HK40 steel is due to the difficulties in the voids coalescing to form the cracks and the difficulty in crack propagation around the lamellar cells. As regards the K3 steel made of the combined addition of Ti and Nb which exhibited the highest creep rupture strength, in addition to the effect of the uniform precipitation of the fine carbides on the strength, the irregular and complex grain boundary morphology of lamellar and massive carbides is assumed to play a very important role in obstructing the cracks from propagation, thus resulting in a longer creep rupture life.

Summary and Conclusion

In this work, the objective of achieving the optimum high temperature strength for the centrifugally cast HK40 steel was approached by controlling the as cast and secondary structures of the steel. The results are summarised as follows:

1. The optimum strength of plain HK40 steel was obtained from the tube with the highest rate during the solidification, so causing the largest dendrite cell structure "d", and it was found that the value of "d" is an important factor for creep rupture strength "σ" i.e. $\sigma \propto 1/\sqrt{d}$.
2. The indicated improvement in creep rupture strength of Ti or Nb added HK40 steels was obtained in the atomic ratio Ti or Nb/C≃0.5 and was correlated with the differences in the grain boundary morphologies in relation to crack propagation as follows:
   a) In addition to the dispersion strengthening effect by the uniform precipitations of secondary carbides caused by Ti addition; the propagation rate of the cracks which forms during the tertiary creep is slow in Ti added steel, due to its discontinuous grain boundary carbide morphology, as compared with the plain HK40 steel, which has a continuous grain boundary carbide morphology. As a result, there is higher total creep rupture life.
   b) In the case of Nb added steel, the cracks propagate through a looped path around and inside the lamellar carbide cell boundaries taking a rather longer time than Ti added steel, thus resulting in longer creep life. It is worthy to note that the number of voids or cracks is not as important as their propagation rate for creep rupture strength.
3. Utilizing the improving effect of the single additions of Ti and Nb, a combined addition of both Ti and Nb was made and gave the highest creep rupture strength. This is considered as an extraordinary improvement for the creep rupture strength of HK40 steel at the higher temperatures. It is obvious from the figures that the creep rupture strength of 0.15%Ti+0.6%Nb added HK40 steel, of the atomic ratio (Ti+Nb)/C=0.26, is about 1.7 times that of the plain HK40 steel if used at the same temperature; and it is nearly the same as that of the plain HK40 steel at the temperature 100 degree C lower. Moreover, it is worth of note that this steel is superior in creep rupture strength to the 1N519 alloy.

References

1. W. Herda and G. L. Swales: Werkstoffe u. Korrosion, 1971, vol.22, p.759.

2. J. Voogd and J. Tielrooy: Hydrocarbon Processing, 1967, vol.46, p.115.

3. B. Estruch and C. Lyth: Material Technology in Steam Reforming processes, pergamon press, (1964), p.29.

4. D. J. Cox and D. E. Jordan: Ibid, p.121.

5. J. F. B. Jackson, D. Slater and D. W. O. Dawson: Ibid, p.153.

6. J. A. Van Echo, D. B. Roach and A. M. Hall: Journal of Basic Eng., Trans. of ASME, 1967, vol.89, p.467.

7. T. Shinoda, T. Ishii, R. Tanaka, T. Mimino, K. Kinoshita and I. Minegishi: Metall. Trans., 1973, vol.4, p.1213.

8. T. Shinoda, R. Tanaka, T. Mimino and K. Kinoshita: Proc. Int. on the Science and Technology of Iron & Steel, part II, 1971, p.1224.

9. T. Shinoda, R. Tanaka, T. Matsuo, T. Mimino and K. Kinoshita: Proc. Int. on Mechanical Behaviour of Materials, III 1972, p.181.

10. G. J. Cox and D. E. Jordan: AFS Trans., 1971, vol.79, p.45.

11. D. B. Roach: Material Protection and Performance, 1972, p.38.

12. BYE. Sadowski: Welding J., 1973, vol.53, p.49-S.

13. D. McLean: Vacancies and Other Point Defects in Metals and Alloys, 1958, (London: Inst. of Metals), Monograph No.23, p.188.